

22 **Abstract**

23 **Background** Estimating the transmissibility of infectious diseases is key to inform situational
24 awareness and for response planning. Several methods tend to overestimate the basic (R_0) and
25 effective (R_t) reproduction numbers during the initial phases of an epidemic. The reasons driving the
26 observed bias are unknown. In this work we explore the impact of incomplete observations and
27 underreporting of the first generations of infections during the initial epidemic phase.

28 **Methods** We propose a debiasing procedure which utilises a linear exponential growth model to
29 infer unobserved initial generations of infections and apply it to EpiEstim. We assess the
30 performance of our adjustment using simulated data, considering different levels of transmissibility
31 and reporting rates. We also apply the proposed correction to SARS-CoV-2 incidence data reported
32 in Italy, Sweden, the United Kingdom and the United States of America.

33 **Results** In all simulation scenarios, our adjustment outperforms the original EpiEstim method. The
34 proposed correction reduces the systematic bias and the quantification of uncertainty is more
35 precise, as better coverage of the true R_0 values is achieved with tighter credible intervals. When
36 applied to real world data, the proposed adjustment produces basic reproduction number estimates
37 which closely match the estimates obtained in other studies while making use of a minimal amount
38 of data.

39 **Conclusions** The proposed adjustment refines the reproduction number estimates obtained with the
40 current EpiEstim implementation by producing improved, more precise estimates earlier than with
41 the original method. This has relevant public health implications.

42

43 **Keywords**

44 Outbreak analysis; SARS-CoV-2; reproduction number; emerging epidemics; EpiEstim method

45

46 **Summary**

47 We propose a back-imputation procedure tackling the issue of unobserved initial generations of

48 infections to reduce the bias observed in the early R_0 and R_t estimates and apply it to EpiEstim using

49 simulated and reported COVID-19 data to evaluate it.

50

51

52

53

54

55

56

57

58

59 Introduction

60 The wide-ranging impacts of the current COVID-19 pandemic have highlighted the threats posed
61 by infectious diseases to our society. The impacts of such threats are not exclusively confined to the
62 domain of public health: in addition to the millions of confirmed deaths worldwide, COVID-19 has
63 caused severe economic and societal disruption around the world.
64 As such, it is crucial that the properties of all emerging pathogens are adequately characterised as
65 soon as possible, making the best use of the limited data that are typically available in the early
66 phases of an epidemic. In particular, understanding the transmissibility of a novel pathogen allows
67 for the evaluation of the risks involved, to inform public health decision making and the
68 implementation of interventions.
69 In this context, the basic and instantaneous reproduction numbers, R_0 and R_t , represent key
70 epidemiological parameters. R_t represents the average number of secondary infections
71 caused by a single infectious individual at time t and R_0 represents the average number of secondary
72 infections generated by a typical infection in a completely susceptible population.
73 These parameters relate to important quantities such as the final size of an epidemic [1] and the
74 critical herd immunity threshold [2,3] and are essential to project the expected future number of
75 cases, hospitalisations and deaths.
76 In the last couple of decades, several methods have been developed to estimate R_t . EpiEstim,
77 developed by Cori et al. [4], has been recommended as one of the best methods for near real-time
78 estimation of R_t to detect changes in transmissibility patterns [5]. However, EpiEstim and other
79 commonly used statistical methods, can suffer from systematic overestimation of the basic
80 reproduction number in the early stages of an epidemic [6]. In the initial epidemic stages, EpiEstim is
81 outperformed by simpler inference methods based on exponential growth [7], which produce
82 smaller bias and better quantify uncertainty in R_0 estimates.
83 Following the theory of exponential growth [7], we propose an adjustment to EpiEstim to account
84 for missing initial generations of infections and use simulated

85 data to test its effectiveness. We show how the adjustment entails a reduction in the bias of both
86 the R_0 and early R_t estimates produced by the original EpiEstim method.
87 Finally, we compare the estimates produced with and without the proposed adjustment on early
88 COVID-19 data in Europe and in the US.

89 Methods

90 Several methods, based upon different frameworks, have been developed to estimate the
91 reproduction number. One of the simplest methods assumes exponential growth of the number of
92 new infections, which can be characterised by applying a simple linear regression on the log-
93 transformed incidence data. Wallinga and Teunis [8] base their methodology on determining
94 likelihoods of chains of infections, White and Pagano [9] use branching process theory,
95 while Bettencourt and Ribeiro [10] base their approach on SIR differential equations. In this work we
96 focus on EpiEstim, the method developed by Cori et al [4], which has been recommended for near
97 real-time estimation [5] and has been applied extensively during the ongoing and past epidemics
98 [11].

99 Despite differences in the mathematical formulations, all methods described above infer R_t or R_0
100 from case incidence data using assumptions on the generation interval or the serial interval
101 distributions. The generation interval is defined as the average length of time between the moment
102 an individual becomes infected and the moment in which they infect a secondary case.
103 Similarly, the serial interval corresponds to the difference between symptom onsets of the primary
104 case and symptom onset of the secondary case. Assuming that infectiousness starts after symptom
105 onset and the infectiousness profile of an individual is independent of the incubation period, the two
106 distributions are equivalent [4]. Therefore, without loss of generality, we focus on the generation
107 interval distribution, denoted w .

108 Exponential Growth

109 One of the simplest methods to characterise the speed of an epidemic, as measured by the growth
110 rate r , is to fit the log-transformed incidence data by linear regression. The growth rate r can then
111 be used to estimate the reproduction number R_0 if the generation interval w is known [12]. When
112 observations with 0 cases are present, linear regression requires the addition of a small constant to
113 each incidence data point, so that the logarithm of each data point is well defined.
114 The assumption of exponential growth is justifiable in a first epidemic period where the proportion
115 of susceptible individuals in a population is large. As more individuals get infected and immunity
116 accumulates in the population, the growth of the number of new cases slows down and deviates
117 from being exponential. A rule of thumb to identify the time window of the exponential growth,
118 proposed by White and Pagano [9] and based on the theoretical work of Ball and Donnelly [13], is
119 that the cumulative number of infected individuals does not exceed the square root of the
120 population size.

121 EpiEstim

122 Cori et al. [4] model observed infections as a Poisson process, where the mean is defined via two
123 quantities: the effective reproduction number R_t , and population infectiousness $\Lambda_t = \sum_{s=0}^n I_{t-s} w_s$.
124 The reproduction number is assumed to remain constant over sliding windows of time with length τ ,
125 allowing for data aggregation over time and reduced variance.
126 Assuming a Gamma prior distribution on $R_{t\tau}$, the posterior distribution is Gamma distributed with
127 parameters:

$$a_{post} = a_{prior} + \sum_{s=t-\tau+1}^t I_s, b_{post} = \left(\sum_{s=t-\tau+1}^t \Lambda_s + b_{prior}^{-1} \right)^{-1}, (1)$$

128 where a and b refer to the shape and scale parameters, respectively. Considering $\tau = 1$ and
129 uninformative priors (i.e. letting a_{prior}, b_{prior} tend to 0) yields the posterior mean:

$$\frac{I_t}{\Lambda_t} = \frac{I_t}{\sum_{s=0}^{t-1} w_s I_{t-s}}.$$

130 Thus we can effectively think of EpiEstim's estimates of R_t as closely related to the ratio between
131 the number of observed infections on day t over the population infectiousness on the same day.
132 Given enough data, this estimator can accurately identify R_t and detect abrupt changes in
133 transmissibility [5]. However, the method can suffer from systematic bias in the initial period of
134 estimation, as described by O'Driscoll et al. [6]. When the first chains of infections are not observed,
135 the estimator will tend to attribute all new cases to the first observed cases, overestimating
136 the reproduction number.

137 EpiEstim - proposed adjustment

138 We propose an adjustment to account for unobserved initial infections and exponential growth
139 similar to the one developed in Dorigatti et al. [14]. Specifically, we assume that the epidemic is
140 growing exponentially to back-impute infections in the period prior to the first observation. Note that
141 this assumption is theoretically justified in the early stages of an epidemic [7], and exponential
142 growth inference methods are between the most accurate in this initial period, as observed in
143 O'Driscoll et al.[6]. Our procedure can be summarised in three simple steps and is visualised in
144 Figure 1. First, we fit a linear model on the log-transformed incidence data to estimate the growth
145 rate, λ , as shown in Figure 1A. Second, we use this linear model to back impute incidence data, prior
146 to the time of the first observed case. In particular, we obtain an estimate of the number of cases for
147 S days, where S is the largest possible generation interval length, i.e., the largest value such that $w_s >$
148 0 . We highlight that it is not necessary to round the output of the inferred number of cases, and
149 estimates lower than 1 should not be removed. Finally, we apply EpiEstim to the extended epidemic
150 curve (including the back imputed incidence data).

151 Simulations

152 To evaluate the effects of our correction, we compared the performance of EpiEstim with and
153 without the adjustment on simulated data. We additionally compared the results to those obtained
154 by fitting a linear exponential growth model, as the performance of our correction strongly depends

155 on the accuracy of the estimates of the growth rate .
156 We used a stochastic SEIR simulator to generate 100 epidemic curves for each R_0 values in {1.5,
157 2,2.5,3}.
158 We considered a large population of 10^6 individuals, and epidemics initiated by 5 initial infections.
159 We assumed 3 days and 3.5 days as the mean times spent in the exposed and infectious
160 compartments respectively, yielding a 6.5 mean generation interval commonly used to model
161 COVID-19 [6].
162 To account for imperfect reporting, we simulated two types of issues commonly affecting the
163 observed data: underreporting and unobserved initial generations of infections. We simulate
164 unobserved initial generations by considering the simulated data from day 15 to day 28,
165 corresponding to two generation intervals worth of data after having missed the first two
166 generations.
167 Further, we simulated under-reporting by considering a constant reporting rate p in {0.15 , 0.3 , 0.5 ,
168 1}. Daily observations were sampled as binomial realisations of true incidence with success
169 probability equal to the reporting rate p .

170 Results

171 Method comparison

172 We fitted the exponential growth, EpiEstim and adjusted EpiEstim methods to the simulated data
173 assuming a Gamma distributed generation interval matching the mean and variance of the
174 generating process (i.e., 6.5 mean generation interval).
175 Figure 2 shows the effect of our adjustment when the reporting rate is 50% and shows that the
176 initial bias observed in the estimates obtained with EpiEstim is strongly reduced by the proposed
177 adjustment, and the mean estimates are comparable with those produced by the
178 exponential growth method. These trends are observed for each value of p , implying consistency in

179 the estimates obtained with different reporting rates (Figure 2 and Supplementary Figures 4 to 6).
180 Our adjustment does not only improve the accuracy of the central estimates of R_0 , but also improves
181 uncertainty quantification. Average credible/confidence interval widths and coverage are reported
182 in Figure 3. Coverage remains constant across different values of the reporting rate for the estimates
183 obtained with the exponential growth and adjusted EpiEstim methods. On the other hand, the large
184 bias observed in the estimates obtained with EpiEstim implies that as credible intervals get
185 narrower, coverage decreases dramatically (Figure 3, panels B and C). The EpiEstim adjustment
186 proposed in this paper produces generally narrower credible intervals as compared to the
187 exponential growth method, at the price of a slight decrease in coverage. This trade-off is in favour of
188 our adjustment for values of R_0 larger than 2, when coverage amongst the
189 two methods is similar. Further, we highlight that the proposed adjustment does not influence later
190 estimates of R_t produced by EpiEstim (Figure 1).

191 Impact of missed generations

192 Beyond simulating undetected cases, reflecting a surveillance system which may be unprepared or
193 unaware of a newly unfolding epidemic, we investigated the impact of the number of unobserved
194 generations on the estimates obtained with our adjustment using simulated data generated under a
195 scenario with perfect reporting rate ($\rho = 1$) and $R_0 = 2.5$. From each epidemic trajectory, we
196 considered 3 different left truncations of the data to account for 0, 1 and 2 unobserved generations.
197 We then applied EpiEstim with and without the proposed adjustment using biweekly time windows
198 starting on weeks 0, 1 and 2.
199 Figure 4 shows the distribution of the mean estimates for the 100 simulations. Each row identifies
200 the number of unobserved generations, while on the x-axis we show the time window used to
201 obtain the estimate.
202 Figure 4 also shows that the adjustment is particularly useful when larger numbers of initial
203 generations are unobserved. While the proposed adjustment produces comparable estimates to

204 those obtained with EpiEstim when all generations are observed (top row of Figure 4), its
205 dependence on the exponential growth method introduces a layer of stochasticity that
206 increases the variance of the mean estimates. On the other hand, when 1 or 2 generations are
207 unobserved, the proposed adjustment adequately compensates for EpiEstim's bias and the median
208 estimates become closer to the true R_0 value used to simulate the data.

209 Application to reported COVID-19 data

210 In addition to validating the proposed adjustment on simulated data, we applied it to real-world
211 COVID-19 incidence case data reported in the John Hopkins Center for Systems Science and
212 Engineering database [15,16]. During the initial phases of the outbreak, surveillance systems of
213 several countries were unprepared to detect infectious individuals and it is likely that the first
214 generations of infections were not observed, justifying our back-imputation adjustment. We
215 selected Italy, Sweden, UK and the US as case studies. For each country, we fitted the log-
216 transformed incidence case count reported for the first sequential 7 days of sustained transmission
217 (no days with 0 new cases in the selected time window) with a linear regression model. We then
218 inferred the number of unobserved cases before the selected time window and applied EpiEstim
219 with and without adjustment to the observed and imputed data, using weekly sliding windows and
220 assuming a generation interval with mean 5.7 days and standard deviation of 1.72 days [17] . Figure
221 5 shows that the adjustment lowers the estimates of R_0 in every scenario, suggesting a role for
222 unobserved generations of infections in overestimating the early R_0 estimates of SARS-CoV-2, which
223 in turn also affect the early estimates of R_t . We obtained average R_0 estimates of 3.6 with 95%
224 credible interval (2.8,4.6) in the UK, 5.2 (95% CrI 4.9,5.6) for Italy, 8.7 (95% CrI 7.8,9.6) for the US and
225 3.9 (95% CrI 3.5, 4.3) in Sweden.

226 Discussion

227 We propose a correction for the systematic overestimation of R_0 that occurs in the early stages of an
228 epidemic when using EpiEstim and other common inferential methods, utilising a back-imputation
229 procedure which relies on exponential growth.

230 The proposed correction aims to account for unobserved generations of infections. For this reason,
231 we deem it to be most applicable in scenarios where generations of infections may have been
232 missed due to emergency situations and limited testing, and generation intervals are relatively short.

233 In practice, the adjustment will prove especially useful to evaluate transmissibility of diseases that
234 are either asymptomatic or cause mild symptoms for a large proportion of infected individuals.

235 Similarly, the adjustment may prove applicable to diseases characterised by long time lags between
236 infection to symptom onset, especially if infectiousness develops significantly earlier than symptoms.

237 In this paper, we demonstrate the application of this adjustment to the EpiEstim method, though it
238 can be applied to other statistical methods where this bias may occur. The resulting adjusted

239 EpiEstim method combines the best features of EpiEstim and the exponential growth method, which
240 is more adequate for the early phases of an epidemic. In particular, the long-run R_t estimates of the

241 original EpiEstim method are preserved, while the initial bias observed in the estimates is reduced by
242 the proposed adjustment. This was confirmed in all scenarios of our simulation experiments,

243 independently of the reproduction number and the reporting rate values used to simulate the data.
244 The adjusted estimates of R_0 strongly outperformed the estimates obtained with the original

245 EpiEstim method in terms of bias and coverage, and produced tighter 95% credible intervals. Our
246 results show that the R_0 estimates obtained with the adjusted EpiEstim and linear exponential

247 growth method are very similar. This is likely due, in part, to the fact that the proposed adjustment
248 relies on linear regression, which is used for the back imputation of the unobserved generations of

249 infections.
250 The proposed method does not currently incorporate uncertainty in the growth rate estimate nor in

251 the imputed cases. Further work is required to understand how the uncertainty in our correction
252 may be best propagated throughout the R_0 or R_t estimation process.

253 The effect of our adjustment was evident when working with early COVID-19 data from Italy,
254 the UK, Sweden and the US. The adjusted estimates were significantly lower than the estimates
255 obtained with the original EpiEstim method, and were found to be largely consistent with estimates
256 derived in Ke et al.[18]. This is especially encouraging considering that our adjusted R_0 estimates
257 were obtained by making use of 7 days' worth of data, while those of Ke et al. [18] were obtained on
258 both case and death time series data spanning months.
259 This suggests that our method can yield improved precision with limited information, which may
260 prove valuable in emerging epidemics. While several papers and meta-analyses reported estimates
261 of the exponential growth rate for the 4 countries [19–21], the parameterisation of the generation
262 interval used and the reproduction number estimates were often lacking [22] thus hindering further
263 comparisons. Further, the adjustment alone was not enough to explain the estimated decrease in R_t
264 in the study period considered (see Figure 5), possibly suggesting that changes in individual
265 behaviour and governmental interventions lowered transmissibility of the disease. However, other
266 biases may be playing a role, such as changes in reporting rates, overestimation due to importations
267 [23], or model misspecification.

268 Critically, the results are sensitive to the choice of EpiEstim parameters, such as the generation
269 interval and the length of the time window used. As expected, longer generation intervals produce
270 larger reproduction number estimates, and we observe larger discrepancies between the estimates
271 obtained with the original and adjusted EpiEstim methods, even if the coefficient of variation is kept
272 constant (Supplementary Figures S1-S3).

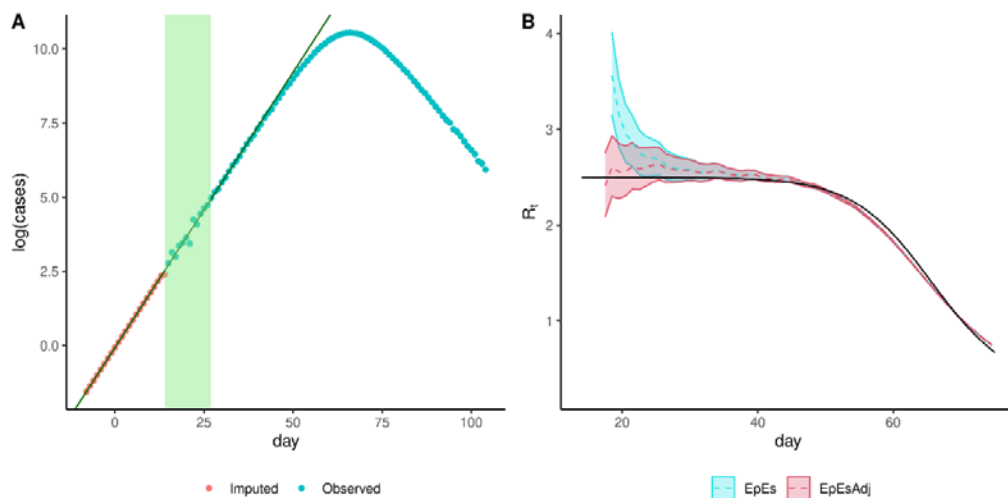
273 Concerning the choice of the sliding window, the larger time windows produce smoother estimates,
274 which reduces the impact of the imputed cases.
275 This means that our adjustment has a much smaller effect when considering sliding windows
276 covering two generation intervals worth of data or more.

277 It is possible that other methods may estimate the initial growth rate more accurately than linear
278 regression particularly if the assumption of exponential growth is not met. In fact, the linear
279 regression model assumes normality of the errors, which may not always hold true with count data.
280 In future work it will be interesting to compare alternative methods to back impute unobserved
281 cases from early incidence data.

282 Here, we have used a linear exponential growth method to infer missing initial generations of
283 infection, improving the accuracy of early R_0 and R_t estimates produced by commonly used statistical
284 methods such as EpiEstim. Our analysis shows how a simple adjustment can reduce initial bias in
285 reproduction number estimates in a newly emerging epidemic when the interpretation of
286 reproduction number estimates is crucial for public health decision making.

287

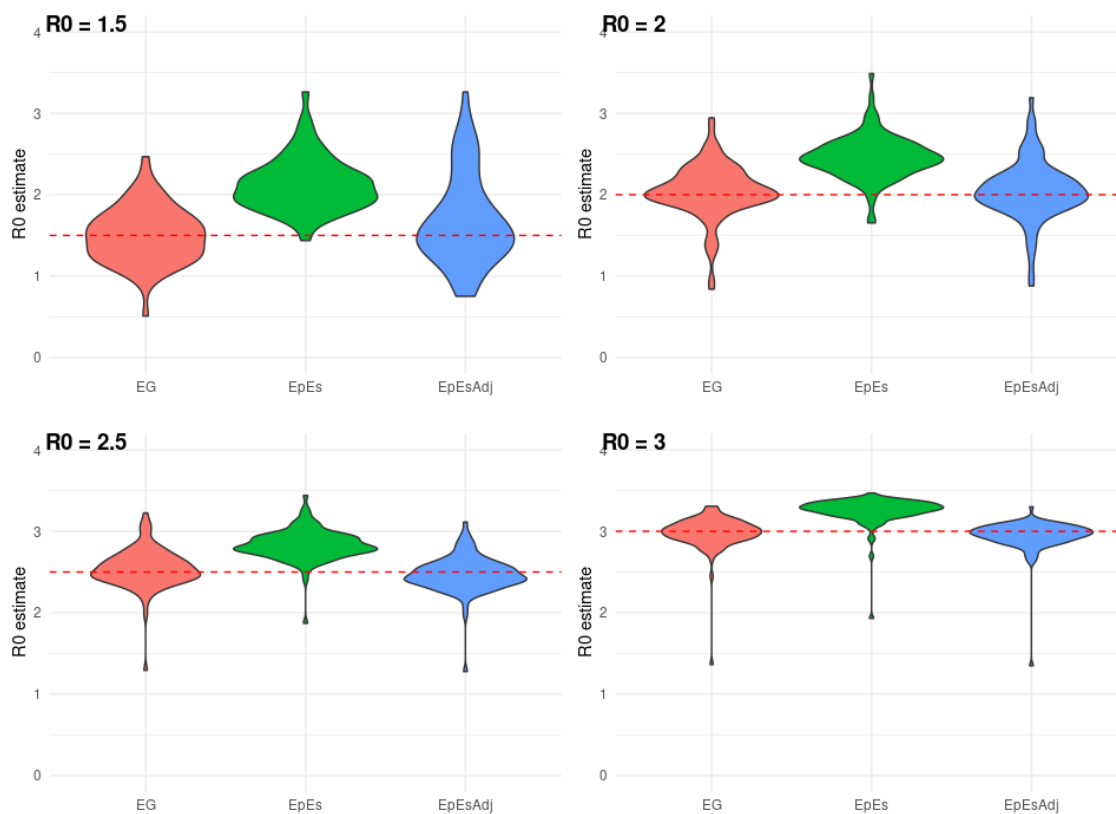
288



289

290 **Figure 1. Visualisation of the exponential growth adjustment method applied to simulated data**
291 **obtained with $R_0 = 2.5$, reporting rate $\rho = 1$ and resulting changes in posterior estimates having**
292 **assumed 2 unobserved generations.** On panel A, the logarithms of the first reported data (those in
293 the green region) are used to fit a linear model (line). The linear model is then used to back-impute
294 unobserved cases (red dots) to complement the available data (blue dots). On panel B, the true R_t
295 value (black solid line) is compared to EpiEstim estimates without (blue) and with (red) adjustment
296 using sliding windows of 7 days. The back-imputation reduces the initial mean estimates (dotted
297 lines) and 95% credible interval widths (ribbons). The adjusted method then converges to the
298 original method as the importance of the imputed datapoints vanishes. Method abbreviations:

299 EpiEstim (EpEs); Adjusted EpiEstim (EpEsAdj)



300

301 **Figure 2. Distribution of mean R_0 estimates assuming a fixed reporting rate $\rho=50\%$.** Each panel
302 shows the distribution of the mean R_0 estimates obtained using 100 simulations for a given true R_0
303 value (red dashed line). Method abbreviations: Linear exponential growth rate method (EG);
304 EpiEstim (EpEs); Adjusted EpiEstim (EpEsAdj).

305

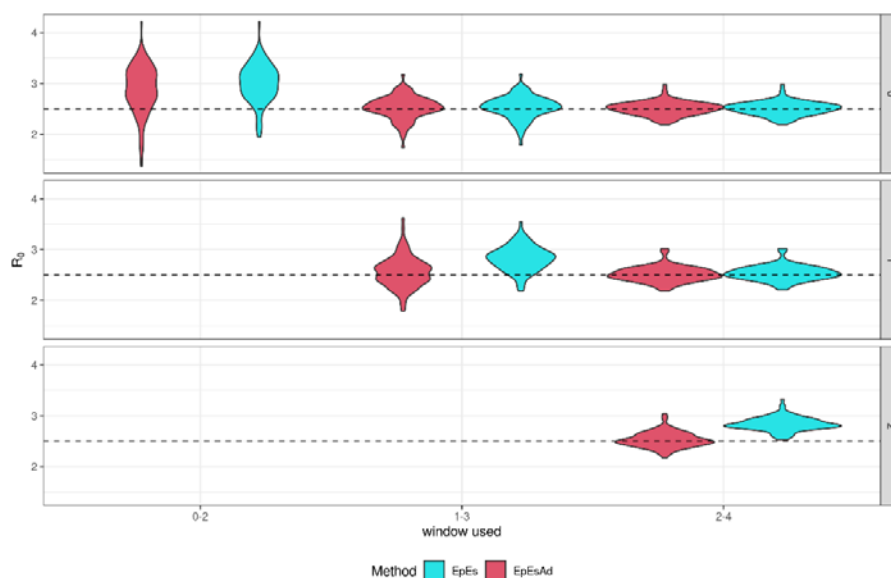
306



307

308 **Figure 3. Median (point) and 95% CrI (interval range) of the basic reproduction number (R_0) mean**
 309 **estimates (panel A), mean coverage (panel B) and mean 95% confidence/credible intervals widths**
 310 **(panel C) for different values of R_0 and reporting rates ρ . Each panel represents distinct values of R_0 ,**
 311 **while different colours represent different reporting rates. Method abbreviations: Linear**
 312 **exponential growth rate method (EG); EpiEstim (EpEs); Adjusted EpiEstim (EpEsAdj).**

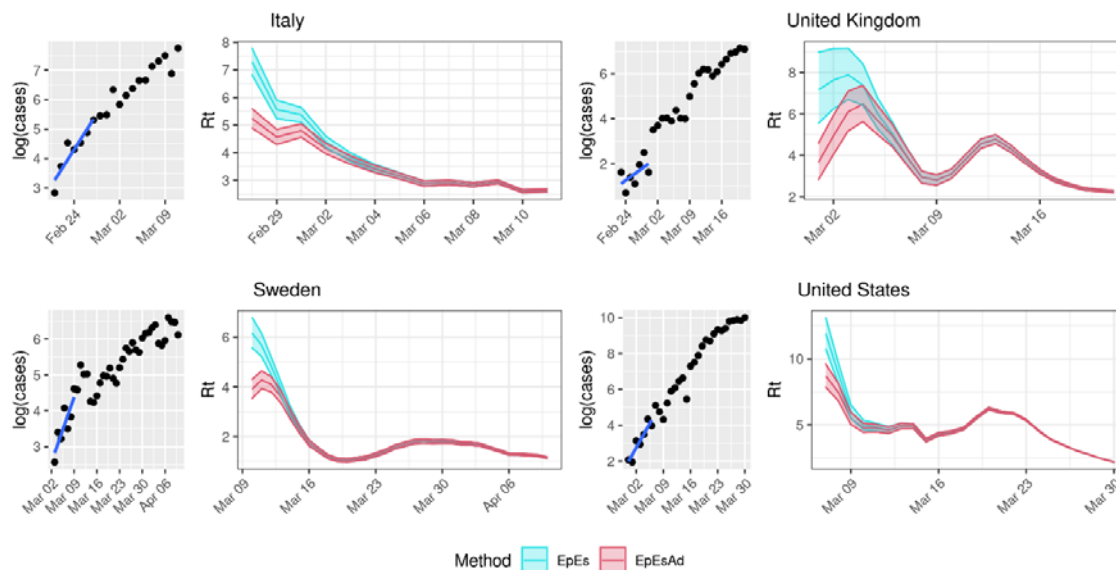
313



314

315 **Figure 4. Distribution of mean R_0 estimates, obtained using biweekly time windows (x-axis) and a**
316 **variable number of unobserved generations (0, 1 and 2, see rows), assuming $R_0 = 2.5$ and reporting**
317 **rate $\rho = 1$. EpiEstim estimates are shown in blue, adjusted EpiEstim estimates are shown in red. On**
318 **the axis, the sliding window used to fit the method is shown. Each window contains 14 consecutive**
319 **data points, starting at week 0, or week 1, or week 2. Method abbreviations: EpiEstim (EpEs);**
320 **Adjusted EpiEstim (EpEsAdj).**

321



322
323 **Figure 5: Comparison of R_t estimates obtained with (red) and without (blue) adjustment for**
324 **COVID-19 data in 4 countries: Italy, France, the UK, and the USA.** Each quadrant includes a
325 subfigure showing the logarithm of the data and the regression line (left) and the R_t estimates
326 obtained using a sliding window of 7 days (and the data up to that day) and a generation interval of
327 mean 5.7 days and standard deviation of 1.72 days (right). Method abbreviations: EpiEstim (EpEs);
328 Adjusted EpiEstim (EpEsAdj).

329
330
331

332 Acknowledgments

333 Funding

334 This work was supported by the Engineering and Physical Science Research Council through the
335 EPSRC Centre for Doctoral Training in Modern Statistics and Machine Learning at Imperial and
336 Oxford. We acknowledge the Abdul Latif Jameel Institute for Disease and Emergency Analytics,
337 funded by Community Jameel and the MRC Centre for Global Infectious Disease Analysis (reference
338 MR/R015600/1) jointly funded by the UK Medical Research Council (MRC) and the UK Department
339 for International Development (DFID), under the MRC/DFID Concordat agreement and is also part of
340 the EDCTP2 programme supported by the European Union. ID acknowledges research funding from
341 a Sir Henry Dale Fellowship funded by the Royal Society and Wellcome Trust [gran 213494/Z/18/Z].

342 Contributions

343 AB, MO'D, ID conceived the study and the methods; AB performed the analysis, developed the code
344 and wrote the first draft; all authors revised and approved the manuscript.

345 Data Statement

346 The data and R code to reproduce this analysis are available on GitHub:

347 https://github.com/abriz97/R0_simulations

348

349

350 References:

- 351 1. Andreasen V. The Final Size of an Epidemic and Its Relation to the Basic Reproduction
352 Number. *Bull Math Biol* **2011**; 73:2305–2321.
- 353 2. Thompson RN, Hollingsworth TD, Isham V, et al. Key questions for modelling COVID-19 exit
354 strategies: COVID-19 Exit Strategies. *Proc R Soc B Biol Sci* **2020**; 287.
- 355 3. Hethcote HW. *The Mathematics of Infectious Diseases*. 2000. Available at:
356 <http://www.siam.org/journals/ojsa.php>.
- 357 4. Cori A, Ferguson NM, Fraser C, Cauchemez S. A new framework and software to estimate
358 time-varying reproduction numbers during epidemics. *Am J Epidemiol* **2013**; 178:1505–1512.
- 359 5. Gostic KM, McGough L, Baskerville EB, et al. Practical considerations for measuring the
360 effective reproductive number, R_t . *PLoS Comput Biol* **2020**; 16:1–21.
- 361 6. O’Driscoll M, Harry C, Donnelly CA, Cori A, Dorigatti I. A Comparative Analysis of Statistical
362 Methods to Estimate the Reproduction Number in Emerging Epidemics, With Implications for
363 the Current Coronavirus Disease 2019 (COVID-19) Pandemic. *Clin Infect Dis* **2020**; :1–9.
- 364 7. Ma J. Estimating epidemic exponential growth rate and basic reproduction number. *Infect.*
365 *Dis. Model.* 2020; 5:129–141. Available at: <https://doi.org/10.1016/j.idm.2019.12.009>.
366 Accessed 14 April 2021.
- 367 8. Wallinga J, Teunis P. Different epidemic curves for severe acute respiratory syndrome reveal
368 similar impacts of control measures. *Am J Epidemiol* **2004**; 160:509–516.
- 369 9. White LF, Pagano M. A likelihood-based method for real-time estimation of the serial interval
370 and reproductive number of an epidemic. *Stat Med* **2008**; 27:2999–3016.
- 371 10. Bettencourt LMA, Ribeiro RM. Real time bayesian estimation of the epidemic potential of
372 emerging infectious diseases. *PLoS One* **2008**; 3.

- 373 11. WHO Ebola Response Team. Ebola virus disease in West Africa—the first 9 months of the
374 epidemic and forward projections. *N Engl J Med* **2014**; 371:1481–1495.
- 375 12. Wallinga J, Lipsitch M. How generation intervals shape the relationship between growth rates
376 and reproductive numbers. *Proc R Soc B Biol Sci* **2007**; 274:599–604.
- 377 13. Ball F, Donnelly P. Strong approximations for epidemic models. *Stoch Process their Appl* **1995**;
378 55:1–21.
- 379 14. Dorigatti I, Okell L, Cori A, et al. Report 4: Severity of 2019-novel coronavirus (nCoV).
380 Available at: <https://doi.org/10.25561/77154>. Accessed 19 April 2021.
- 381 15. Dong E, Du H, Gardner L. An interactive web-based dashboard to track COVID-19 in real time.
382 *Lancet Infect Dis* **2020**; 20:533–534. Available at:
383 [https://www.thelancet.com/journals/laninf/article/PIIS1473-3099\(20\)30120-](https://www.thelancet.com/journals/laninf/article/PIIS1473-3099(20)30120-1/fulltext#.YW1FPhdAlyQ.mendeley)
384 [1/fulltext#.YW1FPhdAlyQ.mendeley](https://www.thelancet.com/journals/laninf/article/PIIS1473-3099(20)30120-1/fulltext#.YW1FPhdAlyQ.mendeley). Accessed 18 October 2021.
- 385 16. COVID-19 Data Repository by the Center for Systems Science and Engineering (CSSE) at Johns
386 Hopkins University. Available at: <https://github.com/CSSEGISandData/COVID-19>.
- 387 17. Ganyani T, Kremer C, Chen D, et al. Estimating the generation interval for coronavirus disease
388 (COVID-19) based on symptom onset data, March 2020. *Eurosurveillance* **2020**; 25:1.
389 Available at: www.eurosurveillance.org. Accessed 10 May 2021.
- 390 18. Ke R, Romero-Severson E, Sanche S, Hengartner N. Estimating the reproductive number R_0 of
391 SARS-CoV-2 in the United States and eight European countries and implications for
392 vaccination. *J Theor Biol* **2021**; 517:110621.
- 393 19. Arif Billah MI, Mamun Miah M, Nuruzzaman Khan MI. Reproductive number of coronavirus: A
394 systematic review and meta-analysis based on global level evidence. **2020**; Available at:
395 <https://doi.org/10.1371/journal.pone.0242128>.

- 396 20. Alimohamadi Yousef Taghdir Maryam SM. Estimate of the Basic Reproduction Number for
397 COVID-19: A Systematic Review and Meta-analysis. *J Prev Med Public Heal* **2020**; 53:151–157.
398 Available at: <http://www.jpmp.org/journal/view.php?number=2072>.
- 399 21. Yu C-J, Wang Z-X, Xu Y, Hu M-X, Chen K, Qin G. Assessment of basic reproductive number for
400 COVID-19 at global level: A meta-analysis. *Medicine (Baltimore)* **2021**; 100.
- 401 22. Spouge JL. A comprehensive estimation of country-level basic reproduction numbers R_0 for
402 COVID-19: Regime regression can automatically estimate the end of the exponential phase in
403 epidemic data. *PLoS One* **2021**; 16:e0254145. Available at:
404 <https://dx.plos.org/10.1371/journal.pone.0254145>. Accessed 8 September 2021.
- 405 23. Mercer GN, Glass K, Becker NG. Effective reproduction numbers are commonly
406 overestimated early in a disease outbreak. *Stat Med* **2011**; 30:984–994.
- 407